RSC Advances

REVIEW

View Article Online
View Journal | View Issue

Cite this: *RSC Adv.*, 2021, **11**, 30657

The intrinsic piezoelectric properties of materials – a review with a focus on biological materials

Ratanak Lay,[ab] Gerrit Sjoerd Deijs[abc] and Jenny Malmström *[ab]

Piezoelectricity, a linear electromechanical coupling, is of great interest due to its extensive applications including energy harvesters, biomedical, sensors, and automobiles. A growing amount of research has been done to investigate the energy harvesting potential of this phenomenon. Traditional piezoelectric inorganics show high piezoelectric outputs but are often brittle, inflexible and may contain toxic compounds such as lead. On the other hand, biological piezoelectric materials are biodegradable, biocompatible, abundant, low in toxicity and are easy to fabricate. Thus, they are useful for many applications such as tissue engineering, biomedical and energy harvesting. This paper attempts to explain the basis of piezoelectricity in biological and non-biological materials and research involved in those materials as well as applications and limitations of each type of piezoelectric material.

Received 7th May 2021
Accepted 7th September 2021

DOI: 10.1039/d1ra03557f

rsc.li/rsc-advances

Introduction

In addition to the rapid technological and social development of our societies, we intensively strive for a healthier life. Both areas are inherently linked; clean and renewable energy sources are needed to keep up with our worldwide demand sustainably and, at the same time, reduce the negative impacts of global warming and environmental pollution. Alternative renewable energy sources such as biomass, solar, wind and tidal energy are helping in the de-carbonization of the power sector.[1–4] Mechanical energy harvesting is one of the front-runners to sustainably power micro-devices. These devices play a key role in our daily lives, not only for leisure but also to an increasing degree for monitoring/adjusting biological systems, including *in vivo* processes.[5–7] This monitoring will be beneficial for diagnostics, for example, real time heart-beat observation,[8] on time medical interventions[9] and ultimately leading to longer and healthier lives.

Mechanical energy harvesting research is gaining momentum, even at the nanoscale range.[10–14] There is plenty of 'wasted' mechanical energy available in the environment waiting to be converted into useful electrical outputs. Daily human activities show possible energy harvesting examples such as talking, walking, running, heart pumping, knee bending, driving vehicles, *etc.*[14–17] A promising way to harvest this wasted

[a]*Department of Chemical & Materials Engineering, Faculty of Engineering, The University of Auckland, Auckland, New Zealand. E-mail: j.malmstrom@auckland.ac.nz*
[b]*MacDiamid Institute for Advanced Materials and Nanotechnology, Wellington, New Zealand*
[c]*Department of Chemistry, Faculty of Science, The University of Auckland, Auckland, New Zealand*

Ratanak Lay holds a Bachelor of Chemical & Materials Engineering from the University of Auckland. For his fourth-year project, he undertook research to investigate the effect of teeth's exposure to coke on its mechanical properties. His passion for biology and materials engineering pushed him to pursue higher education in Master of Engineering, where he joined Dr Jenny Malmström's research group to investigate the piezoelectric properties of Bovine tendon collagen and apo-haemoglobin fibrils.

Sjoerd Deijs is a bio-molecular scientist with broad experience in biotechnologies. His broad experience range from assay development and research into Covid-19 immunity tests to characterization of biopiezoelectricity.

ambient mechanical energy is by using piezoelectricity. Piezoelectricity can provide a possible sustainable contribution, as part of a bigger solution scheme to the sustainability issues. It can help to minimise the reliance on non-renewable energy sources and ensure a more efficient use of natural resources.

Piezoelectric research started off by focusing on inorganic materials such as zinc oxide (ZnO),[10] barium titanate ($BaTiO_3$)[18] and lead zirconate titanate ($Pb_xZr_{1-x}TiO_3$, known as PZT),[19] but it later branched out to organic polymer materials such as polyvinylidene fluoride (PVDF) and polymer composites.[20] In 2006, Wang *et al.* reduced the size of a ZnO piezoelectric device to create a nanogenerator. In this work, nanowires were deformed by small forces, which induced electrical charge generation at the lower and upper parts of the nanowires, confirming the possibility of using piezoelectricity for energy harvesting.[10]

Piezoelectricity is not only present in inorganic compounds, but it also plays a crucial role in biological organisms.[21] It has been reported that piezoelectricity exists in various biological structures ranging from amino acids to tissues, and some of them have comparable piezoelectric strength to that of conventional piezoelectric materials.[22] Furthermore, organic piezoelectric materials such as collagen hold several advantages over conventional piezoelectric ceramics including biocompatibility, biodegradability, high flexibility, low toxicity, and ease of fabrication.[23]

Piezoelectricity in biological structures has already been explored to fabricate energy harvesting nano-generators.[24] However, its biggest potential lies within biomedical applications, due to relatively low energy demands and a need for biocompatible materials. Currently, batteries power various implantable devices that need to be replaced at the end of their lifespan. This requires surgery which can impose risk or complication to the patient.[22] To overcome these limitations, it would be ideal to take advantage of energy that is wasted during the natural processes of the body. The origin of bio-piezoelectricity and its role in the biological structure are currently not fully understood, this impedes the development of bio-piezoelectric applications. Large heterogeneity within biological structures also limits precise control of the polarization's strength and direction.[25] Therefore, understanding the mechanisms behind piezoelectricity in biological structures is key to developing and optimizing their applications further.

This review complements other published reviews on the topic[21,26–29] by providing a careful examination of literature to gain a better grasp of the underlying mechanism of piezoelectricity with a particular focus on biological materials. It also attempts to provide a summary of key piezoelectric biological and traditional materials, their differences, applications and limitations, as well as a brief overview of the current state of piezoelectric development. This review provides a resource for the basic understanding of piezoelectricity to aid further development of piezoelectric applications in the future.

Jenny Malmström is a senior lecturer at the Department of Chemical and Materials Engineering at the University of Auckland. She is a Principal Investigator of MacDiarmid Institute for Advanced Materials and Nanotechnology. Her research focusses on creating functional biointerfaces to understand and control biological systems, but also on how to use biological materials or bio-inspired strategies to create functional materials.

Fundamentals of piezoelectricity

Piezoelectricity is a linear electromechanical coupling phenomenon.[30] This means that when mechanical stress is applied to a piezoelectric material, it deforms and generates electrical charges. The process of converting mechanical stress to electrical charge is known as the direct effect. In contrast, the converse effect refers to when an external electrical field is applied across a piezoelectric material causing the material to mechanically deform.[30] Piezoelectricity exists in materials with non-centrosymmetric crystals. Out of the 32 crystal classes, 21 of them of lack a centre of symmetry and are said to be non-centrosymmetric and thus are piezoelectric.[31]

Piezoelectricity is quantified by the piezoelectric coefficient d, which is the ratio between applied stress and charge (eqn (1)), or between strain and applied electric field (eqn (2)).

$$P = \frac{Q}{A} = dX \tag{1}$$

$$x = dE \tag{2}$$

where P is the polarization (C m^{-2}), Q is the charge (C), A is the area (m^2), d is the piezoelectric coefficient (C N^{-1} for the direct effect and m V^{-1} for the converse effect), X is the stress (N m^{-2}), x is the mechanical strain (unitless) and E is the electric field (V m^{-1}).[32] As the piezoelectric coefficient is a third-tank tensor, in the direct piezoelectric effect, eqn (1), the polarisation is a vector and the stress is a symmetric second-rank vector. In the converse piezoelectric effect, eqn (2), the electric field is a vector while the strain is a symmetric second-rank tensor.[33]

The piezoelectricity of a material depends on both the orientation and symmetry of the material's crystal, and it can be described by third-rank tensors.[32] The piezoelectric tensor can be expressed as a 3×6 matrix of component $d_{ij,}$ where i represents the direction at which electrical field is applied or produced, and j represents the direction of applied stress or resulting strain.[31] The subscripts 1–3 are used to represent X, Y and Z directional axes, and subscripts 4–6 are used to describe the shear planes perpendicular to each of those axes respectively. Since piezoelectricity is a direction-dependent property, the piezoelectric coefficient d has both magnitude and direction. The positive/negative sign indicates the direction of the

resulting strain or induced polarization in respect to their reference axis.

For inorganic materials, the piezoelectricity is a result of asymmetrical charge distributions in the crystal under applied mechanical stress.[30] The piezoelectricity of inorganic materials shows temperature dependent behaviours. Above a critical temperature known as the Curie temperature, a material dissipates its piezoelectric and ferroelectric properties.[34] In other words, thermal motions can induce changes in the polarization of the material. On the other hand, piezoelectricity in organic materials arise mainly from reorientation of permanent molecular dipoles under an applied stress that results in alignment of the dipoles in a particular direction that yields a net polarization.[23]

Inorganic piezoelectricity

Single crystalline ceramics. Traditionally, piezoelectric materials were divided in two groups: piezoelectric single crystals and polycrystalline ceramics. In 1880, the Curie brothers were the first to identify quartz as a piezo-electric crystal.[35] After this initial finding, a noticeable alternative, Rochelle salt (or potassium sodium tartrate tetrahydrate), was discovered in 1922 and found to exhibit a higher piezoelectric strength than that of quartz.[36] This salt was substituted by the introduction of ammonium dihydrogen phosphate (ADP) crystals.[37] After ADP, synthetic efforts produced the first $BaTiO_3$ (barium titanate) piezoelectric crystal.[18] Owing to different ferroelectric phases in titanate, their piezoelectric effect is considerably higher when compared to quartz.[38] In ferroelectric materials, the polarization magnitude and direction can be altered by an application of external electric field (at $T < T_c$, where T_c is the Curie temperature).[39] The remaining polarization after electric field application removal is called permanent polarization (hysteresis), and upon mechanical pressure this permanent polarization generates the piezoelectric output. Recently, zinc oxide (ZnO) has received particular interest as a sustainable piezoelectric material. ZnO produces hexagonal piezoelectric crystals which have a low dielectric constant and room temperature ferroelectricity.[13,40,41] This metal oxide has a piezoelectric effect due to an asymmetrical wurtzite crystal structure and large electromechanical coupling capabilities.[42] When ZnO is fabricated in a nano-rod/wire configuration, it has a heightened sensitivity due to a large surface to volume ratio which makes it a great material for sensors.[43,44] Wang *et al.* fabricated a ZnO piezoelectric nanogenerator (NG) based on aligned ZnO nanowires.[10] Even though the NG output was initially just enough to run a nanodevice, such as a molecular electronic memory device,[45] ZnO nanogenerators have undergone a lot of development, and now show a stunning piezoelectric coefficient of $d_{33} = 512$ pC N^{-1}.[46] To achieve such high piezoelectric coefficient, a wet chemical co-precipitation method was used to dope ZnO nanorods with neodymium. The nanorods were subsequently mixed with polydimethylsiloxane (PDMS) and spin coated to interface with electrodes. To gain a finger tap ($\sim$0.3 N per tap) output grasp; the undoped ZnO NRs showed $\sim$2 V *vs.* $\sim$31 V Nd–ZnO NRs.[46] Although single crystals have been very influential piezoelectric materials, they are somewhat overshadowed by the performance of polycrystalline ceramics. For example, the single crystal $BaTiO_3$ has piezoelectric coefficient d_{33} of $\sim$86 pC N^{-1},[18] while the polycrystalline ceramic $BaTiO_3$ shows $\sim$350 pC N^{-1}.[47]

Polycrystalline ceramics. Polycrystalline ceramics possess many crystal structures that are randomly orientated and only become functional after a polarization step. This often includes the application of a high electrical field to align the material's dipole moments through a process known as electrical poling.[48] The structure of the ceramic material is influenced by the synthesis methods, which are generally divided into wet chemistry methods such as sol–gel, and solid-state synthesis.[49] Wet chemistry methods generally have the advantage of more efficient mixing, producing more homogenous materials and significantly lower calcination temperature when compared to solid-state synthesis. Despite these advantages, solid-state synthesis is the most commonly used synthesis method due to its ability to produce ceramics with better piezoelectric properties and being less complex than wet chemistry methods.[49]

Well known piezoelectric ceramics include lead zirconate titanate (PZT),[50–52] barium titanate ($BaTiO_3$)[18,47,48,53] and potassium sodium niobate ($K_{0.5}Na_{0.5}NbO_3$, abbreviated as KNN).[54–56] The high piezoelectric potential of PZT is what makes it a particularly attractive energy harvester (d_{33} = 500–600 pC N^{-1}).[57,58] It also exhibits ferroelectricity as observed by characteristic hysteresis loops. However, the brittle nature of PZT limits its applications. It is prone to fractures due to a high Young's modulus of 50 GPa and a tensile strain maximum of 0.2%.[59] Practical testing under applied electric fields have indeed shown a tendency of PZT fatigue cracking in a brittle process with little or no plastic deformation.[60] Owning to the high strain demand for converting ambient energy, energy harvesting devices must be both flexible and stretchable. Therefore, piezoceramics, such as PZT, are combined (often in a film configuration) with plastic or elastomeric substrates.[50,52,61] One method utilized printing of PZT onto a pre-strained PDMS and created buckled PZT nano-thick ribbons upon release of the strain.[61] This buckled PZT showed an order of magnitude larger strain endurance when compared to the flat non-treated PZT.[61] Even though these composite devices are more durable, other mechanical properties should also be examined as it is still possible that slipping, cracks and delamination occurs.[62] In addition, one major downfall of PZT is that it contains lead, which is not only toxic, but also environmentally unfavourable.

An alternative lead free piezoceramic is $BaTiO_3$, another ferroelectric material. The piezoelectric capabilities of $BaTiO_3$ were discovered in the early 1940s and the material was soon considered as a potential piezoelectric transducer.[63] However, it was initially over-shadowed by PZT which showed better piezoelectric properties and a higher T_c.[64] $BaTiO_3$ came back into the picture when modifications of $BaTiO_3$ with Ca^{2+} and Zr^{4+} enabled an increase of the piezoelectric coefficient to d_{33} > 500 pC N^{-1} with a maximum operational temperature of 90 °C.[65]

Several characteristics, for instance; crystallization,[66] calcification,[67] sintering,[67] changing grain size,[68] poling[48] and doping[69] can be used to enhance piezoelectric properties. Recently, one of the key piezo-enhancement factors have been identified to be morphotropic phase boundaries which are the transitions in the composition phase diagram, where the crystal structure changes rapidly and where the electromechanical properties are maximised.[39,70] By carefully exploring such phase boundaries and optimising materials accordingly by varying chemical composition or mechanical pressure, it is possible to enhance the electromechanical coupling further.[19,38,54] In one study of the morphotropic phase boundaries in $BaTiO_3$-based ceramics, it was found that a high d_{33} (700 ± 30 pC N^{-1}) could be induced in a specific region while in a broad range it showed >600 pC N^{-1}.[53] Even at the temperature between 10–40 °C, the optimised $BaTiO_3$ surpassed the performance of popular lead-based systems.[59] These steps make the employment of $BaTiO_3$ for electronics more feasible. One crucial remaining factor that requires improvement for $BaTiO_3$ is to increase the Curie temperature (about 130 °C for pure $BaTiO_3$). To increase the Curie temperature, one recent study combined a ceramic ($BaTiO_3$ + bismuth ferrite $BiFeO_3$) with bismuth aluminate $BiAlO_3$ (BA) with a high T_c of 527 °C.[70] This study achieved an increase of the piezoelectric constant from $d_{33} = 97$ pC N^{-1} to 210 pC N^{-1} and a T_c of 400 °C.

As a result of a high Curie temperature and an impressive piezoelectric coefficient, KNN is another candidate to replacing PZT.[55] Saito *et al.* demonstrated a d_{33} of 416 pC N^{-1} for KNN in 2004 by discovering a morphotropic phase boundary of the material and by processing into highly textured polycrystals.[54] Optimisations, such as tailoring the phase fraction and chemical modifications[71–73] have since produced KNN-based materials with even higher piezoelectric constants. However, KNN-based materials are also hampered by fatigue deterioration, an area where there is still a lot to be discovered and optimised for this material (reviewed by Genenko *et al.* 2015).[74]

Organic–inorganic metal halide perovskites (OMHPS)

Perovskites are materials with the crystal structure of calcium titanate which is known as the perovskite crystal structure.[75] They consist of two cation types bonded together by an anion. Organic–inorganic metal halide perovskites (OMHPs) consist of; an organic cation (A), a metal cation (B) and a halide anion (X) with the general formula of ABX_3.[76]

Instead of the high fabrication temperature of ceramics, a low temperature OMHP fabrication was achieved with TMCM–$MnCl_3$ (TMCM = trimethylchloromethyl ammonium). With ferroelectric properties, piezoelectric output of $d_{33} = 185$ pC N^{-1} and a T_c of 132 °C it is attractive for several applications.[77] Further morphotropic phase boundary research resulted in a superlative OMHP with a d_{33} of ~1540 pC N^{-1} consisting of trimethylfluoromethyl ammonium (TMFM), TMCM and $xCdCl_3$ (x = different composites).[78]

Another interesting OMHP capability, namely illumination dependent piezoelectric response, was found in a methylammonium lead halide ($MAPbI_3$) in which the piezoelectric output varied with different illumination.[79] It was suggested that the illumination enhances the $MAPbI_3$ dielectric constant and forms a considerable photo-induced piezoelectric dipole,[79,80] which could play a role in energy harvesting by perovskite solar cells.[76] Despite of the high piezoelectric output, the same ceramic disadvantages apply for OMHP; they show brittleness, inflexible properties when in bulk form. To overcome these limitations future studies could use thin film configurations on flexible substrates.

Organic piezoelectricity

Organic molecules such as polymers can exhibit complex dipole moments giving rise to polymer-based piezoelectricity.[81,82] Polymers are excellent materials for piezoelectric devices due to; low-cost solution processing, low temperature processing, low toxicity and high chemical stability.[83] This review divides piezoelectric polymers in two classes, namely bulk polymers (which normally require poling) and polymer composites.

Bulk polymers. Bulk polymers generally require mechanical stretching and poling to exhibit significant piezoelectricity. The applied electrical field affects the orientation of positive and negative charges and dipoles and consequently induces piezoelectricity.[81] This class of piezoelectric polymers mainly includes poly(vinylidene fluoride) (PVDF), PVDF copolymers and polyimides.

Piezoelectricity of PVDF was first reported in 1948, followed shortly after by reports of piezoelectric co-polymers of PVDF.[84] PVDF is a polycrystalline (35–70% crystallinity) polymer with mainly ''head-to-tail'' arrangement of polymer chains in a zigzag form in the crystal grains. Consequently, dipoles are parallel to one another within adjacent chains.[85] This dipole moment is what leads to the piezoelectricity in PVDF. There are four crystal forms of PVDF: α, β, γ and δ, with α being the simplest form to obtain. Unfortunately, only the β form has a piezoelectricity of ~30–40 pC N^{-1}.[82] Despite this relatively low output, the intrinsic properties of PVDF creates an opportunity to overcome the disadvantages of bulk inorganic piezoelectric devices. These include: simple synthesis,[86] high flexibility,[87] and adaptable design.[88] Fig. 1A shows the output voltage and the flexibility of a PVDF based thin film on a cellulose paper substrate.[87] The device exhibited a maximum open circuit voltage of 1.5 V under periodic bending and releasing of force at ~1 Hz.[87]

As the β form is the crystal with the most prominent piezoelectricity, studies are focussing on increasing the amount of this form. Frequently used improvement methods are: stretching,[89] polar additives[87] and electro-spinning.[20] One of the most promising PVDF copolymers explored for piezoelectric properties is PVDF-*co*-TrFE (trifluoroethylene). This copolymer is interesting because it demonstrates a higher piezoelectric power density (312.85 μW cm^{-3})[90] when compared to PVDF (81.3 μW cm^{-3}).[91] The TrFE monomer adds an extra fluorine to the polymer, which induces a higher tendency for β form formation.[92] PVDF-TrFE has been used in energy harvesters by spin coating,[90] electro-spinning[93–95] or bar coating[91] of the polymer. The processing and deposition parameters of the

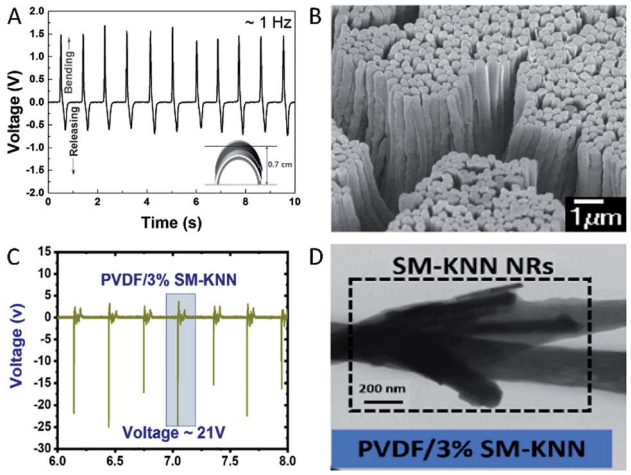

Fig. 1 PVDF based piezoelectric devices (A) open-circuit voltage of a flexible PVDF-TrFe thin film energy harvester. Reproduced from ref. 87 with the permission of AIP Publishing. (B) PVDF-TrFE nano-array formation. Reproduced from ref. 97, with the permission of Springer Nature. (C) Open-circuit voltage of PVDF/SM-KNN energy harvester. (D) TEM image of the PVDF/SM-KNN composite. Reproduced from ref. 108, with permission from Elsevier.

polymer are varied to optimise the β crystal phase formation and thus increase the piezoelectric output.[90] Electrospinning into nanofibers has been found to further increase the piezoelectric power density output of the polymer.[96] During electrospinning, a high bias electric field is applied which leads to dipole alignment along the major axis direction of the nanofibers.[96,97] Aligning PVDF-TrFE into a nanotube array (Fig. 1B) has also been shown to induce higher piezoelectric output (d_{33} = −35 pm V^{-1}) when compared to conventional spin coated films (d_{33} = −17.8 pm V^{-1}).[97] All in all, PVDF-TrFE is a promising flexible polymeric material, not only for piezoelectric energy harvesting but also as pressure sensors[98] and actuators.[99]

Amorphous polymers with high glass transition temperatures (T_g > 80 °C) are being studied for their piezoelectric responses as an alternative for high temperature processes. At the glass transition temperature, the amorphous polymer shifts from a glassy brittle state (limited molecular motion) to a flexible rubbery state (large scale molecular motion). Amorphous polymers generally rely on oriented dipole moments for their piezoelectricity.[100] Such orientation is achieved by poling near the T_g. Examples of amorphous polymers explored for their piezoelectric properties are co-polymerized pyromellitic dianhydride with *p*-phenylenediamine[81] and co-polymerized vinylidene cyanide and vinyl acetate.[101]

Polymer composites. Polymers are often explored as composites with other piezoelectric materials such as ceramics, metal oxides and salts.[88,102–105] These composites benefit from an increasing flexibility when compared to ceramics, while retaining relatively high piezoelectric performance.[106,107] Generally, higher piezoelectric output is obtained upon increasing the ceramic content. This content is often in the form of nanofiller, optimized in terms of concentration and distribution uniformity. Well known fillers are: barium titanate ($BaTiO_3$), potassium sodium niobate (KNN), metal oxides and salts.[88]

As an example of a successful composite, Mota *et al.* used rotating-disk electrospinning technique to create composite PVDF/$BaTiO_3$ thin fibre meshes. The fibre alignment could be altered by changing the rotation speed, which was also found to change the amount of the piezoelectric β phase of the PVDF.[106] The composite was also optimised in terms of composition and the authors achieved a 130 pC N^{-1} piezoelectric output at a 20/80 $BaTiO_3$/PVDF composition.[106] The authors additionally demonstrated preliminary evidence of biocompatibility in *in vitro* experiments, making this material interesting for use as implantable energy harvester.

PVDF/potassium sodium niobate (KNN) has also been successfully used as a piezoelectric composite. In one example, KNN nanorods were surface functionalised to form a composite with PVDF. The incorporation of rod-shaped KNN nanomaterial (Fig. 1D) was found to positively influence the number of dipoles aligned during electro-spinning.[108] The optimised material contained 3% KNN and a fabricated nanogenerator of this was found to generate an output of ∼21 V (Fig. 1C) and ∼22 μA (compared to control PVDF: 0.5 V and ∼1 μA).[108]

Piezoelectricity in biological materials

It is thought that piezoelectricity of biological materials has physiological importance. For example, it has been shown that the piezoelectricity of bone influences its remodelling and growth according to Wolff's law, which describes the direct correlation between bone's structure and the stress that it is subjected to.[109,110] In fact, it has been confirmed experimentally that under mechanical deformation, bone produces hydroxyapatite mineral, confirming that piezoelectricity in bone is linked to bone growth and remodelling.[111] Piezoelectricity in the lung's elastin has been proposed to have a role in binding oxygen to haemoglobin during respiration.[112] It is also believed that piezoelectricity plays a role in the nervous system for sensing external stimulation.[113] Proteins such as collagen, elastin, actin and myosin have been shown to be piezoelectric.[112,114–120] Their piezoelectric properties have been attributed to their constituent amino acids, electrical dipoles and the packing of the peptide chains.[21,109,121] A summary of the reported piezoelectric coefficients for some protein/amino acid based biological materials is provided in Table 1.

Cellulose. The plant kingdom is a rich source of aligned materials and there has been a long-standing interest in cellulose as a piezoelectric material. This interest stems from the known, albeit weak, intrinsic piezoelectricity of wood.[122,123] While individual cellulose chains have a clear dipole, cellulose microfibrils in plant cell walls are aligned in an anti-parallel fashion, leading to a cancellation of the macroscopic dipole moment.[124,125] Following the evidence of a large permanent dipole moment in cellulose nanocrystals[126] much effort has been devoted to extract and to align/order these into materials with bulk piezoelectricity. Rajala *et al.*[127] produced films of cellulose nanofibrils and found that even without deliberate polarisation or alignment, the fabricated piezoelectric sensors

Table 1 Reported piezoelectric coefficients from various biological materials from amino acid crystals and single proteins to tissues and virus

Direction	Source	Piezoelectric coefficient	Measurement techniques
Longitudinal d_{11}	γ-Glycine single crystal[121]	1.7 pm V^{-1}	Piezometer
Longitudinal d_{22}		−1.1 pm V^{-1}	
Longitudinal d_{33}		9.93 pm V^{-1}	
Shear d_{16}	β-Glycine microcrystals[121]	178 ± 11 pm V^{-1}	Resonance methods
Longitudinal	Tetragonal lysozyme aggregated film[109]	19.3 pm V^{-1}	PFM
Longitudinal	Tetragonal lysozyme aggregated film[115]	3.16 pC N^{-1}	Piezometer
Longitudinal	Monoclinic lysozyme aggregated film[115]	0.94 pC N^{-1}	
Longitudinal d_{31}	Rat tail collagen[140]	−4.84 ± 2.96 pm V^{-1}	PFM
Longitudinal d_{33}		0.89 ± 0.08 pm V^{-1}	
Shear d_{14}		−12.00 ± 2.60 pm V^{-1}	
Shear d_{15}		6.21 ± 2.93 pm V^{-1}	
Shear	Bone collagen[141]	0.1–0.3 pm V^{-1}	PFM
Longitudinal and shear	Murine lung elastin[112]	0.1 pm V^{-1}	PFM
Longitudinal	Human teeth enamel[142]	0.30 ± 0.04 pC N^{-1}	PFM
Longitudinal	Human teeth dentine[142]	0.51 ± 0.05 pC N^{-1}	PFM
Unspecified	Human eyes[143]	23 pC N^{-1}	Rheolograph solid
Longitudinal d_{33}	Wild type M13 bacteriophage monolayer[144]	0.30 ± 0.03 pm V^{-1}	PFM
Longitudinal d_{33}	4E engineered M13 phage monolayer[144]	0.70 ± 0.05 pm V^{-1}	PFM
Longitudinal d_{33}	Lateral aligned M13 phage film[144]	7.8 pm V^{-1}	PFM
Longitudinal d_{33}	Vertically aligned M13 phage film[145]	10.4 ± 0.5 pm V^{-1}	Quasi-static
Longitudinal d_{33}	Vertically aligned M13 phage film[146]	13.2 pm V^{-1}	PFM

exhibited a sensitivity of films in the range of 4.7–6.4 pC N^{-1}. To increase ordering, methods such as mechanical stretching and electrical-field polarisation have been trialled.[25,128,129] One particularly interesting approach was tested by Chae *et al.*[130] They reported a method to induce remarkable parallel packing of bacterial cellulose microfibrils during the bacterial culture by applying directional shear stress *via* rising bubbles. Cellulose based electroactive paper (EAPap) has received significant attention, with a measured piezoelectric coefficient (d_{31}) as high as 1425 pm V^{-1}.[131] Nanocellulose has also been used in composite materials with other biological[132,133] and standard piezoelectric polymers.[134] Recent reviews cover nanocellulose production[135] and piezoelectricity in more detail,[25,136,137] while this review focusses more on protein-based piezoelectric materials.

Amino acids crystals. Amino acids are the building blocks of proteins that serve many important physiological functions in the body. Thus, piezoelectric properties of amino acids, at the nanoscale, are fundamental for understanding the piezoelectric properties of tissues and organs at the macroscale. Out of the 20 natural occurring amino acids, 19 belong to chiral symmetry groups implying that they crystallize in at least two optical isomer forms and lack a crystal symmetry, thus piezoelectricity is their inherent material property.[121] In fact, every amino acid except for methionine has been confirmed to be piezoelectric experimentally.[138,139] The only non-chiral amino acid glycine, crystallises in three polymorphs: α, β and γ-forms.[121] The three forms can interconvert into each other depending on the conditions, in particular in response to humidity. The glycine molecules within an α-crystal arrange in anti-parallel conformation and so the resulting crystal is not piezoelectric.[147] Only the β- and γ-forms have been found to be piezoelectric. However, the β-form has been shown to be metastable and it has the tendency to convert into the γ-form which has been found to be the most stable form under ambient conditions.[147]

A common trend in biological materials is that the shear piezoelectric coefficient is typically higher than the longitudinal piezoelectric coefficient.[109] This is also true for the amino acid crystals. The high shear piezoelectricity in amino acid crystals has been attributed to their relatively low elastic modulus as they tend to be softer when compared to inorganic crystals.[109] This is because the piezoelectric strain coefficient is represented as the ratio between the piezoelectric charge coefficient and the elastic stiffness coefficient.[109] Glycine and hydroxyproline crystals have been found to have the highest piezoelectric coefficients amongst the natural occurring amino acids.[28] The shear piezoelectric coefficient of β-glycine crystals d_{16} has been measured to be as high as 178 pm V^{-1} when measured using piezometer.[121] Such a high shear piezoelectricity was shown to be a result of efficient packing of glycine molecules within the crystal, enhancing the strength of electrical dipoles acting along a certain crystallographic direction.[109] On the other hand, the longitudinal piezoelectric coefficient d_{22} of β-glycine was reported to be only around −5.7 pm V^{-1}.[121] The longitudinal piezoelectric coefficient d_{33} of γ-glycine is around 10 pm V^{-1}, as measured by piezometer.[121,147,148] In addition, ferroelectricity has also been demonstrated experimentally for both of the β- and γ-forms at the nanoscale using density functional theory (DFT), molecular dynamics and PFM.[147,148] The ferroelectricity is higher in the γ-form due to more efficient arrangement of the amide group, which results in accumulation of dipole moment along the polarisation direction.[147] However, the ferroelectricity starts to decrease at 630 K and disappear completely at 640 K as

the glycine molecule transitions from being ferroelectric to paraelectric.[147]

Hydroxy-L-proline has the second highest shear piezoelectric coefficient d_{25} among the amino acids of around −28 pC N^{-1}. And similar to glycine, hydroxy-L-proline is also ferroelectric and so its piezoelectric coefficient can be strengthened by applying an external field to align the polarization domains.[109] Amino acids exhibit structural dependent piezoelectric properties.[21,109,149] By adding –OH groups to proline to generate hydroxy-L-proline, the piezoelectric coefficient of it increases by two orders of magnitude.[109] Hydroxy-L-proline and threonine were found to have no piezoelectricity in the longitudinal direction as single crystals, but when prepared as polycrystalline films, they were demonstrated to have a piezoelectric coefficient d_{33} of 1 pC N^{-1} and 0.1 pC N^{-1} respectively. It was proposed that the resultant longitudinal piezoelectricity in polycrystalline films is a result of inter-crystalline strain within the film which lowers the crystal symmetry of constituting single crystals making the polycrystals overall piezoelectric. In this case, the magnitude of the piezoelectricity is the vector summation of the piezoelectricity of strained randomly oriented single crystals that make up the films.[149]

Proteins. Because of the inherent piezoelectricity of amino acids, many proteins are also found to exhibit piezoelectric responses. Collagen is the protein most widely studied for its piezoelectric properties.[150] Type-I collagen is the most abundant form of collagen, and this form can be found in muscle, skin, bone and tendon.[21,151,152] In fact, collagen I comprises about 25–30% of the total protein in the human body making it the most abundant protein.[12] The collagen structure is made up of three twisted polypeptide chains, each made up of repetitive unit of GPX where G is glycine, P and X are usually proline and other amino acids such as alanine and hydroxyproline.[21] At the ends of each polypeptide, a carboxyl-terminal and an amino-terminal are found, resulting in an electrical dipole along the long axis of the collagen molecule.[150] As stress is applied, the collagen chains reorient themselves causing the dipoles to align along a certain direction that yields piezoelectricity.[23] Although, there is no established theory on the mechanism of piezoelectricity in collagen, it is commonly believed that piezoelectricity in collagen is a result of the strong dipole moment along the peptide chain axis and supramolecular interactions *via* hydrogen bonding.[25,150,153] The highest piezoelectric coefficient measured in collagen corresponds to 12 pm V^{-1}.[140] Using DFT, it has been predicted that the major amino acids in collagen: glycine, proline, hydroxyproline and alanine are all piezoelectric.[109,154] Thus, the piezoelectricity may be related to the vector summation of the constituent amino acids in a direction. In fact, when looking at the tripeptide glycine-hydroxyproline-alanine, the longitudinal piezoelectric coefficient was found to be 0.88 pC N^{-1}, similar to that of collagen when measured using PFM.[109,140] Fig. 2C shows the PFM amplitude image of single collagen fibril. It appears that the piezoresponse shows periodic features that may be related to the physical structure of collagen fibril.[153]

Another widely studied fibrous protein is elastin. It can be found in organs such as lung, skin and blood vessel walls.[112,117,118,150] Both piezoelectricity and ferroelectricity has been confirmed in elastin.[112,117,118] The piezoelectric coefficient of elastin has been found to be 0.1 pm V^{-1}.[112,117] While this is lower than that of collagen, elastin is ferroelectric while as collagen is not, and thus electrical poling can be used to enhance elastin piezoelectric strength. Similar to collagen, the piezoelectricity of elastin originates from its monomers, dipole moments and supramolecular packing.[112]

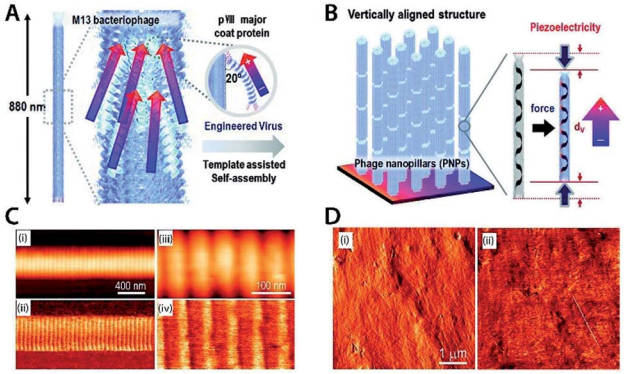

Fig. 2 (A) Structure of M13 bacteriophage. (B) Piezoelectricity in the vertically aligned M13 phage structure. Reproduced from ref. 145, with the permission of Royal Society of Chemistry. (C) AFM topography image (top) and PFM amplitude image (bottom) of single collagen fibril. (D) AFM topography image (left) and PFM amplitude image (right) of bone. Reproduced from ref. 153, with the permission of American Chemistry Society.

Lysozyme, a major globular protein in egg white and mammalian secretions has also been found to exhibit piezoelectricity. The longitudinal piezoelectric coefficient of tetragonal lysozyme monoclinic crystal measured using PFM was found to be 19.3 pm V^{-1}, a relatively high value for biological material.[116] However, since the lysozyme crystal belongs to the (422) crystal group, only shear piezoelectricity is permitted according to the classical theory of piezoelectricity.[115] The origin of the measured longitudinal piezoelectricity was proposed to be a result of a structural defect that lowers the crystal symmetry of the crystal resulted from the crystal preparation.[116] In addition, the longitudinal piezoelectric coefficient of a monoclinic lysozyme crystal film was found to be only around 0.94 pC/N, which is much lower than that of a tetragonal crystal.[115] And because only limited number of studies have been performed on lysozyme, it is difficult to verify the accuracy of the measured values and whether the measured value was indeed deducted solely from piezoelectricity.

Tissues/organs. Bone is a natural composite of approximately 65% hard mineral (hydroxyapatite) and about 35% protein (mainly collagen) by mass.[155] There is a general consensus that the collagen in bone contributes to most of the bone's piezoelectricity.[141,155,156] There is yet no conclusive evidence that the apatite crystals present in bone is piezoelectric.[155] Various studies have been conducted to investigate the piezoelectricity in raw, demineralised and decollagenised bones to investigate each constituent's electromechanical properties of the bone composite.[141,152,156] These studies found that both

raw and demineralised bone exhibited piezoelectricity, but that the piezoelectric coefficient in the demineralised bone was higher than that in bone confirming that bone's collagen is indeed piezoelectric.[141,155,157] The PFM amplitude image (Fig. 2D) shows that the piezoresponse from bone shows similar periodic structure to that in collagen. It was proposed that the lower piezoelectric coefficient in bone was due to the fact that bone is a bio-composite with apatite crystals embedded within collagen matrix. When bone is subjected to an external electric field, the strain produced from the converse effect is distributed onto both the crystals and collagen resulting in a lower effective response from the collagen.[156] The shear piezoelectric coefficient in bone quantified by PFM has been found to be within the range of 0.1–0.3 pm V^{-1}, about two orders of magnitude lower than that in collagen.[140,141,153] The shear piezoelectric coefficient d_{14} was found to be the highest coefficient for both bone and demineralised bone. For decollagenised bone, the piezoresponse measured by PFM from the apatite crystals was found to be only slightly above the background noise level making it difficult to differentiate the two signals and conclude if the apatite crystals contributes to the overall piezoelectricity of bone or not. On the other hand, XRD and dynamic measurements all suggest that the apatite crystals in bone may belong to crystal point groups that are piezoelectric highlighting the discrepancy between measurement methods used and the lack of a standardised method to test for piezoelectricity in biological materials.[155]

Similar to bone, teeth are also a bio-composite mainly comprised of hydroxyapatite nanocrystals and collagen with similar ratio to that of bone, though the piezoelectricity of teeth has not been studied as extensively as in bone. Out of the few studies done on teeth, most assumed that the hydroxyapatite is not piezoelectric as it belongs to the centrosymmetric spatial group $P6_3/m$.[93,152] However, by studying human teeth enamel and dentine after removing collagen, Reyes-Gasga and others have shown that the hydroxyapatite is piezoelectric at both macroscale and nanoscale, but to a much lesser extent compared to collagen.[142] It is possible that the hydroxyapatite present in teeth exists in more than one spatial group. It has been known that hydroxyapatite can also exists in the non-centrosymmetric $P6_3$ and $P2_1$ spatial groups and thus are piezoelectric.[142] The other two teeth tissues, cementum and dentine have been shown to exhibit piezoelectricity across all the studies done on them but the piezoelectric coefficients vary quite significantly between studies.[93,142,152] The nanoscale piezoelectric coefficient for teeth enamel and dentine have been measured by PFM to be 0.3 pC N^{-1} and 0.5 pC N^{-1} respectively.[142]

Tendon is comprised of highly ordered crystalline collagen. And just like any collagen-based material, the shear piezoelectric response is higher than that in the longitudinal direction for both macroscale and nanoscale measurements. In addition, the piezoelectric coefficients measured at the nanoscale using PFM have been found to be an order of magnitude higher than those measured at the macroscale.[119,120,140,156] The shear piezoelectric coefficient d_{14} of rat tail tendon measured at the nanoscale was found to be -12 pm V^{-1}, whilst the longitudinal piezoelectric coefficient d_{33} was measured to be 0.89 pm V^{-1}.[140] The shear piezoelectric coefficient d_{15} in bovine Achilles tendon has been found to be 1 pm V^{-1}, significantly lower than that in rat tail tendon, likely due to the structural arrangement of the collagen fibres not being as efficiently packed as in rats.[140,158]

Sclera and cornea are two other collagen-based tissues in eyes. Just like other collagen-based tissues, their piezoelectricity is strongly dependent on the orientation at which pressure is applied.[143,159,160] The piezoelectric coefficient for a middle circumferentially-cut sclera tissue has been found to be as high 23 pC N^{-1}.[143] But when the sclera tissue is cut in the anterior-posterior position, the piezoelectric coefficient was only around 7 pC N^{-1}.[143] It has also been found that regions with relatively higher elastic modulus corresponds to lower piezoelectricity as it is more difficult to deform mechanically stiff regions.[160] In addition, it has been proposed that the water molecules in collagen help stabilise the structure. Thus, as the tissue dehydrates, the collagen fibres become disoriented which results in a reduction of piezoelectricity.[143,159,160]

Various parts of fish such as swim bladders and scales have been experimentally demonstrated to be piezoelectric.[12,113,161] The fish swim bladder's source of piezoelectricity was attributed to be the self-aligned and ordered collagen nanofibrils.[12,161] The same was said for the *Catla catla* fish scale.[12,161] But the piezoelectricity in green carp scale was said to be from the hydroxyapatite crystals present in the fish scale. Interestingly, both of the *Catla catla* fish swim bladder and scale were found to be ferroelectric as suggested by the characteristic shape of the hysteresis loop.[161] However, ferroelectricity was not demonstrated in collagen in other experiments.[150] This suggest that piezoelectricity in both tissues may potentially also arise from other proteins in addition to collagen. Furthermore, the piezoelectric coefficient for both swim bladder and scale from the *Catla catla* fish were found to be higher than that of isolated collagen nanofibril. The enhanced piezoelectric coefficient was attributed to be a result of cooperative electromechanical interaction between the highly ordered packed and oriented collagen nano-fibrils under applied mechanical stress in both tissues.[12,161]

Piezoelectricity is not unique to animal tissues; it also exists in plants. For example, the longitudinal piezoelectric coefficient of electrically poled aloe vera films has been found to be -6.3 pm V^{-1}, higher than that in collagen.[162] The proteins and polysaccharides in *Aloe vera* plants were said to be responsible for the plant's overall piezoelectricity.[162] Orange peel, a bio-waste that contains cellulose, polysaccharides, proteins and flavonoids has also been found to be piezoelectric.[163] However, piezoelectricity in plants has not been as extensively investigated as in animals. Thus, further research is required to investigate the mechanisms and behaviours of plant piezoelectricity.

Virus. Virus particles are enveloped by proteins and often display a high degree of order and symmetry. Essentially, they provide a self-assembly of proteins, just as collagen fibers do – but using different proteins and producing different shapes. The M13 bacteriophage is an example of a virus that has been found to exhibit piezoelectric properties. It is a long rod shaped

virus covered with ~2700 copies of major coat proteins (pVIII). Five copies of minor coat proteins (pIII and pIX) can also be found at either end of the rod (Fig. 2A).[144,145] The major coat proteins have been suggested to be responsible for the piezoelectricity of the M13 bacteriophage. These proteins have an α-helical structure with a permanent dipole pointing from the amino- to the carboxyl-terminal. When a mechanical stress is applied to the phage, the electrical dipoles align, which results in spontaneous polarisation (Fig. 2B). The phage exhibits piezoelectricity in both axial and radial directions; though the piezoelectric strength is stronger in the axial direction.[144–146] Similar to other biological materials mentioned, the piezoelectricity in the phage shows structural dependency.[145,146] To investigate this, the M13 bacteriophage has been assembled into films in both lateral and vertical directions. In addition, negatively charged glutamate were also inserted into the genetic sequence of the major coat proteins to modulate their piezoelectricity.[144–146] As a result, the self-assembled genetically engineered vertical phage film's piezoelectric coefficient was measured to be between 10.4 to 13.2 pm V^{-1} depending on the preparation technique.[145,146] The higher value was achieved by better mechanical scaffolding from chemical cross-linking and better adhesion of the rod to the substrate.[146] On the other hand, the lateral aligned film had a piezoelectric coefficient of 7.8 pm V^{-1}, lower than that in the vertical aligned phage film. And it is likely because the polarisation in the axial direction is stronger than that in the radial direction.[144]

Applications of piezoelectric materials

This section focusses on examples of different piezoelectric materials being used in applications. As the amount of papers on piezoelectric applications is immense,[164] a handful of applications have been selected to represent the field.

Inorganic and non-biological organic materials. Currently, piezoelectric materials are being used in a wide range of fields including automobiles, architectures, biomedical, electronics and military.[165] First off, piezoelectric materials are incorporated in the animal body to generate energy and to monitor physiological conditions. Excellent incorporation examples come from using piezoelectric material to harvest energy from the natural relaxing and contracting movements of heart, diaphragm and lung.[9] More specifically, a PZT based piezoelectric energy harvester was placed on the epicardial sites of bovine and ovine hearts. When this harvester was combined with rectifiers and micro-batteries, it produced enough output to power a non-stop cardiac pacemaker.[9] Li *et al.* demonstrated a non-lead (ZnO) piezoelectric device which similarly uses heart movements to produce electric outputs.[8] Another incorporated device by Cheng *et al.* used a PVDF thin film to produce a self-powered sensor for blood pressure monitoring (Fig. 3A). This self-powered sensor was wrapped around a porcine ascending aorta and could harvest biomechanical energy (Fig. 3B).[166] The generated pulsating output voltage was shown to be highly linear and sensitive to blood pressure, as to be expected from piezoelectricity. This device reduces the gap for implementing

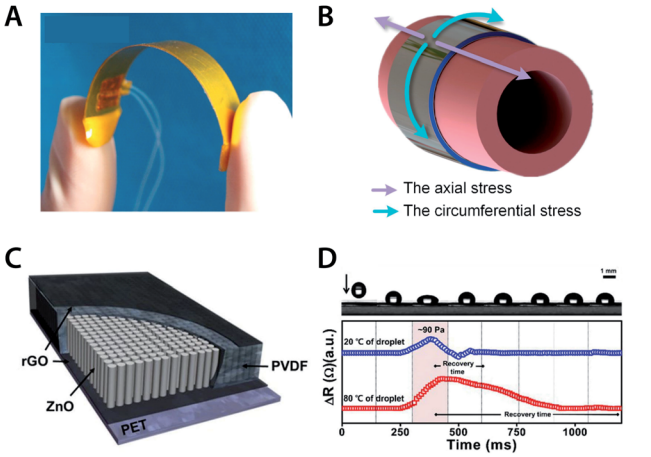

Fig. 3 (A) Self-powered PVDF thin film based blood pressure sensor. (B) Circumferential and axial stress on aorta wall. Reproduced from ref. 166, with permission from Elsevier. (C) Schematic design of ZnO/PVDF based pressure and temperature sensor. (D) Top graph: mechanical impact of droplet onto sensor with unknown temperature. Bottom graph: corresponding resistance and recovery time upon impact of different temperature droplets. Reproduced from ref. 173, with permission from Springer Nature.

a continuous and real-time monitoring system for patients, especially those with hypertension.[166]

Traffic-induced vibrations are another source of 'wasted' mechanical energy of interest for piezoelectric energy harvesting applications. Transportation infrastructures have been modified to hold piezoelectric devices and use the deformations and vibrations from moving vehicles to harvest energy.[167,168] Examples of road infrastructures that have implemented such energy harvesting include railway,[169] road pavement[167] and walk pavement.[170] Even though these projects are still in the experimental phase, piezoelectricity is becoming more commonly utilized in the transportation infrastructures. Interestingly, piezoelectric devices are also experimentally used as transducers to monitor damage in materials, for example, the steel rods in reinforced concrete.[171] To achieve that, an ultrasonic transducer (emission) and a piezoelectric PZT transducer (receiver) were fixed to each end of the steel rod. The rod damage can then be assessed by analysing the change in ultrasonic amplitude, since the amplitude of the ultrasonic wave decreases gradually with the rod damage.[172]

Another example of interesting piezoelectric applications is temperature and pressure sensing. Lee *et al.* demonstrated a temperature/pressure sensor using a composite ZnO/PVDF film (Fig. 3C). To detect the pressure, the change in piezo-resistance of the material was measured. This piezo electrical resistance occurs upon application of mechanical stress (Fig. 3D). To detect the temperature, the recovery time of the piezo-resistance was measured and linked to temperature (Fig. 3D).[173] The device was capable of detecting pressure differences of as little as 10 Pa within a measurement range of 10–140 Pa. Temperature could be measured in the range 20–120 °C.[173]

Finally, it is worthwhile to highlight sensory applications using piezoelectricity in robotics. The robotic field desires to mimic the flexibility and tactile capabilities of biological skin with electronic skin (e-skin). To even be considered for use as an e-skin, the material must be highly flexible and be superior in its ability to adapt to shape. An example of e-skin was made of electrospun PVDF, doped with graphene oxide and $BaTiO_3$ nanoparticles.[174] In this case the authors demonstrated the ability to accurately identify the shape of a hand touching the e-skin and the motion of human joints which might aid in the development of 'smart' prostheses.[174]

Biological piezoelectric materials. Similar to other piezoelectric materials, piezoelectricity in biological materials have also been exploited, or shown to have potential, in various applications. However, due to the high heterogeneity in biological structures and lack of understanding of the mechanism in bio-piezoelectricity, biological piezoelectric materials have not been exploited as extensively as inorganic piezoelectric materials. Despite that, bio-piezoelectricity has already been used to produce nano-generators, supercapacitors, sensors, optical devices and tissue regeneration scaffolds.[23,175] When compared to inorganic materials, bio-piezoelectric materials hold several advantages including biocompatibility, biodegradability, high flexibility and relatively simple processing routes which do not require initial toxic compounds.[23,176] Many biological materials are also able to degrade or decompose into basic molecules such as water or carbon dioxide in physiological conditions without triggering intense immunogenic responses, a crucial requirement for biomedical applications.[165] Furthermore, biomaterials such as fish scale, onion skin cells and eggshell membranes are cost-effective and sustainable sources of piezoelectricity as they are consumed in large quantity and they are currently considered as bio-wastes.[12] By using those bio-wastes, it will also help in reducing the amount of wastes that go into landfills.

Due to their biocompatibility and biodegradability, bio-piezoelectric materials have particular potential as functional materials for biomedical and green energy niches.[23] Various bio-based nano-generators have been fabricated to utilise to the direct piezoelectric effect to generate electricity.[12,162,177,178] Those nano-generators (Fig. 4A–C) exploit the piezoelectricity in abundant biological materials or bio-waste, such as onion skin cell,[14] eggshell membrane,[178] orange peel,[163] aloe vera gel,[162] fish swim bladder,[179] fish scale,[12] bacteriophage and so on.[144,146] Nanogenerators offer several benefits over conventional energy conversion techniques including ease of fabrication, high portability, high conversion efficiency and high sustainability.[23] Nanogenerators can be used to harvest mechanical energy from various forms such as finger pressing, sound, walking and other simple motions that would be otherwise wasted as heat.

Fish scale is one example of a material with energy harvesting potential. Ghosh and Mandal demonstrated that up to 4 V of voltage could be produced under compressive stress of 0.17 MPa using a bio-piezoelectric nanogenerator fabricated from fish scale, which is rich in type-I collagen.[12] Egg shell membrane, another collagen-rich biomaterial, has been used to fabricate a nanogenerator (Fig. 4C) which was able to produce up to 26.4 V per unit under 81.6 kPa of compressive stress. When connected in series and parallel, five units produced a total of 131 V, enough to power more than 90 green LEDs.[178]

In addition to being successfully used to fabricate nano-generators, collagen and collagen-based materials have been experimentally demonstrated that they can be used for various other biomedical and tissue engineering applications. Fish-skin collagen and gelatine were used to produce biosensors in the form of e-skin to monitor physiological signals that may provide information regarding medical conditions.[180,181] Interestingly, those sensors could be powered by nano-generator produced from the same materials proving their ability to function as self-powered devices.[180–182] Collagen also has the potential for tissue engineering applications as tissue scaffold and wound-healing dressing.[183] It has been known that bio-piezoelectricity relates to growth and remodelling in tissues such as bone, hence it would be beneficial to exploit the piezoelectricity in materials such as collagen to develop tissue scaffolds that help promote a self-healing environment for wounds.[180,181] Furthermore, collagen applications extend beyond biomedical applications and have been used to produce sensors measuring physical properties such as humidity and strain.[182,184]

As for the M13 bacteriophage, it has been used to fabricate nano-generator,[144,146] sensor,[185] and tissue engineering scaffolds.[186,187] The phage is particularly versatile owing to its well-defined structure, narrow size distribution and the ability to modify the phage's properties with genetic and chemical modifications.[144,145] Most importantly, the phage can be mass produced simply by infecting bacteria in culture where the phage co-opt the bacteria's metabolism releasing millions of its copies overnight.[144] The ability to modify the phage's properties and ease of production might make the phage a more feasible option than the other materials mentioned.

One of the main challenges for bio-piezoelectric applications is that piezoelectric coefficients of biological materials are relatively low when compared to their inorganic counterparts.[23] They can be modified or processed to enhance their

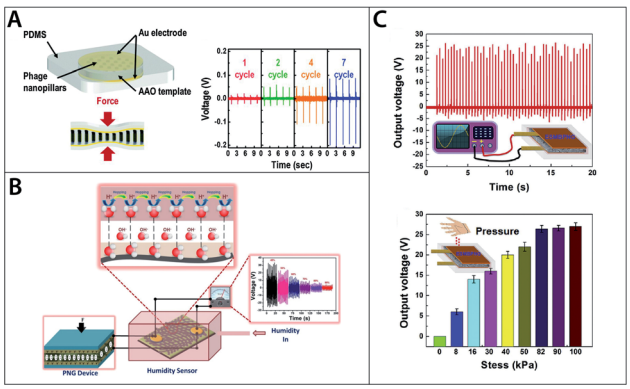

Fig. 4 (A) Schematic of M13 bacteriophage based energy generator and generated voltage outputs. Reproduced from ref. 145, with permission from Royal Society of Chemistry. (B) Schematic of self-powered collagen-based humidity sensor. Reproduced from ref. 182, with permission from ACS publication. (C) Output voltage for eggshell membrane based energy generator. Reproduced from ref. 178, with permission from Elsevier.

piezoelectric strength for more energy intensive applications. For example, collagen has a relatively low longitudinal piezoelectric coefficient. However, it has been shown that cross-linking with EDC-NHS allows for the collagen fibres to self-assemble into a bundle more efficiently, with enhanced piezoelectricity in the longitudinal direction as a result.[151] Electrospinning of chitin nano-fibre is another example of how processing can be used to improve material properties. In this case, the electrospinning was found to increase the crystallinity, and thereby the piezoelectric strength by 400%.[188] Alternatively, bio-piezoelectric materials can also be combined with conventional piezoelectric materials such as PVDF to enhance their piezoelectricity.[163] Gaur *et al.* combined the bio-waste orange peel with PVDF and produced a hybrid nanogenerator that was able to produce an output voltage of 90 V, three times higher than that of pure orange peel alone.[163]

Discussion/limitations

While piezoelectric materials are used in numerous applications already, there are still some challenges left to solve. The high piezoelectric output of lead-based piezoceramics (*e.g.* PZT) have made these materials a benchmark. However, it is important to note that even the best piezoelectric materials provide very low energy density compared to energy harvesting technology such as solar and wind. Therefore, the applications where piezoelectric energy harvesting is suitable are those where not much power is needed, and where other types are not practical. One such example is to power implanted medical devices with sensor capabilities. The most efficient, lead-based piezoceramics are also problematic environmentally, and have in fact been banned in many applications.[189,190] Therefore, much of the research and optimisation of PZT based devices have been applied to non-lead ceramics. Consequently, several non-lead piezoceramics such as ZnO, $BaTiO_3$ and KNN have gained momentum. However, as bulk materials they do not surpass PZT output. With complex modifications, non-lead ceramics can be competitive and occasionally even surpass lead-based ceramics.[56,66–69]

For both lead and non-lead ceramics, the achieved output in volts is not the limiting factor; however, the current output is. Widespread application of piezoelectric energy harvesters is restricted due to this low current output. While volts transcends into the 100 V region, the reported current output is generally in the nano–micro amperages range.[67,88,90,107] Consequently, enhancing this current output remains one of the toughest challenges. One possible solution to this problem is to manufacture piezoelectric devices in a multi-stacking design on a flexible substrate to use it as a bending energy harvester.[191,192] In addition, time should be spent on creating a load and source impedance that are corresponding to each other. This impedance matching will aid in minimizing the losses of the energy harvesting.[192,193]

It could be argued that non-lead modified piezoceramics, in terms of piezoelectric output, are ready to be the benchmark in the electronics world. But while some of these materials have sufficient output, their inherent nature of being brittle and fragile still holds them back for certain applications. Especially biomedical applications need flexibility and stretchable energy harvesters due to energy conversion from soft tissues. The energy harvester should not only be completely adaptable to target organs or skin but also not restrict tissues in their normal function.[166] In other words, no excessive strain should be created.

A possible solution for both flexible and stretchable energy harvesters may be found in biological piezoelectric materials. Piezoelectricity in biological materials have many potential applications in electromechanical, bio-medical and other areas. Even though these materials are flexible and stretchable, several factors still limit the development of biological piezoelectric applications. The main limiting factors are the lack of understanding of bio-piezoelectricity and a large discrepancy between experimental results from a pool of limited number of conducted experiments. The discrepancy between experimental could be a result from the lack of standardised testing method for bio-piezoelectricity which underpin development of bio-piezoelectricity.[111] The understanding of the inherent properties and mechanism of piezoelectricity in each material is vital to reach an optimised device.

Various studies have quantified piezoelectric coefficients for biological materials at structural levels ranging from the amino acid level to tissue or organ level. Compared to traditional piezoelectric ceramics, piezoelectric coefficients for each biological material span over a much wider range, sometimes over several orders of magnitude.[21,25,165] Since piezoelectricity is a material intrinsic property, the piezoelectric coefficient of a material measured at a condition should be consistent.[25] A large discrepancy in the measured values from biological materials in particular raises a question of whether the reported piezoelectric coefficients originate solely from the piezoelectric properties of each material. Piezoelectricity is not the sole intrinsic electromechanical coupling process in a material. Electrostriction and flexoelectricity are the two other electromechanical coupling process that may interference with the measurements.[25,150] Piezoelectricity couples mechanical and electrical domains of a material in a linear manner. Like piezoelectricity, electrostriction in a dielectric material is the deformation under an applied electric field. However, unlike piezoelectricity, electrostriction is a quadratic electromechanical coupling and it can occur without having the permanent dipoles aligning across all domains.[25,150] Flexoelectricity is the polarisation induced in a dielectric material by a strain gradient. Unlike piezoelectricity, flexoelectricity is a size-dependent phenomenon and it is less prominent in a bulk material as it is relatively harder to induce a strain gradient in a large material.[25,150] In addition, extrinsic factors such as ion migration and electrostatic interactions may also affect the measurements especially for hydrated samples.[25,150] Since the direct and converse piezoelectric effects are thermodynamically equivalent, they can be measured to confirm if the measured value indeed truly corresponds to the piezoelectricity of the material.[26] However, due to technical limits, especially in nanomaterials, this may not always be possible. The converse effect can be, and has been, quantified at the nano-level using PFM,

but it is challenging to quantify the direct effect at such scale as the detection sensitivity of currently existing instruments are not high enough to detect the low output signals from biological materials.[25] In addition, noise signals, such as Johnson noise and contact electrification, can sometimes be as large or greater than the signals from the piezoelectricity themselves.[25,165] This has been exemplified from measurements on hydroxyapatite crystals in bone. Although XRD and dynamic measurements both suggest that the crystals are piezoelectric, as they belong to a non-centrosymmetric crystal group, PFM results are inconclusive as the measured signals were barely above the background noise.[155] It is therefore extremely important that the right sample preparation method and measurement technique are used to identify the electromechanical phenomenon so that the correct mechanism can be correctly identified for the development of its application.

Another available option to overcome the flexibility disadvantage of ceramics is using flexible piezoelectric polymers (often PVDF and its co-polymers) or creating composites of ceramics (often in nanoparticle form) and polymers. Optimisation and sometimes complex fabrication steps are needed to create a decent balance between mechanical characteristics and electrical output.[106–108,194] Even though PVDF and its co-polymers are great options to increase flexibility of the composites, effort also needed to be directed towards increasing the β phase quantity in PVDF. Numerous studies have combined PVDF with a nanofiller non-lead piezoelectric ceramic.[104–107] However, as shown by Bairagi *et al.*, the hydrophobicity of PVDF does not always match with the polarity of chosen ceramics.[108] Future studies should take the compatibility of PVDF or other polymers into account and optimize it to their chosen ceramic. While on the subject of PVDF compatibility, some piezoelectric devises use hydrophilic and rigid electrodes, for instance, Cu, Ag or Au based.[82,89] Comparatively hydrophilic electrodes may suffer from surface contact issues, which affects the total energy harvesting capabilities. Rigid electrodes also suffer from mechanical issues, such as easy crack formation upon deformation and eventually breakage.[74]

The substrate supporting the piezoelectric material or film, also must be taken into consideration. In particular, in terms of flexibility. Common substrates, such as Pt/Si, Pt/Ti/SiO_2/Si and Pt/TiO_2/SiO_2/Si are not flexible and are prone to cracks and breakage. Techniques that uses flexible polymers or fabrics as a sort of substrate are less prone to inflexibility problems.[106,195] An alternative flexible substrate is a hybrid paper containing for example conducting polymers, multi-walled carbon nanotubes or ionic liquids for conductivity and the migration of ions.[196] Flexible polyethylene terephthalate (PET) sheets[107] have also been used for PVDF piezoelectric devices.

Another challenge lies in matching of the piezoelectric device with energy storage devices. For example, in energy harvesting from organs, the output pulses will be in sync with the pulsing organ. Consequently, energy storage is often needed. All the components of the total device should be investigated for long-term mechanical and chemical stability (protection against rust or oxidation). Not only *in vitro* but especially *in vivo*.

In vivo experiments are crucial for piezoelectric clinical applications and should not only focus on stability but predominately on biological safety, including implantation safety. As surgery is always a challenge for the body (anaesthesia, incisions, suturing and risk of infection) it is essential that a piezoelectric device and its components do not interfere with the normal functioning of the body. This can, for example, be investigated with inflammatory response or cytotoxicity tests *etc.*[197] Many clinical applications would also benefit from linking a piezoelectric device with a wireless signal transmitting system such as telemetry.[7] There are numerous examples of biological systems that are desirable to monitor real time. For instance, hypertensive patients would benefit a lot of a self-powered piezoelectric blood pressure sensor[166] combined with a telemeter which transmits the signal to monitoring equipment.

Since piezoelectricity in a material is strongly affected by the material's structure, piezoelectricity at the nanoscale does not necessarily translate into piezoelectricity at the microscale. In principle, the alignment of polar domains leads to stronger piezoelectricity. Thermodynamically however, a random arrangement is favourable, which leads to randomly oriented polar domains being more common in nature.[25,31] It is also important to note, that same material may be strongly piezoelectric at the nanoscale, but not at the microscale. This would be the case if the polarisation domains are randomly oriented at the micrometre length scale, leading to a reduction or cancellation of net polarisation.[25] Most piezoelectric ceramics are ferroelectric, thus electrical poling can be used to align polarisation domain direction to enhance the strength of the polarisation. Most biological materials however are not ferroelectric, and electrical poling is not applicable. Methods like mechanical stretching have the potential to induce alignment in biological materials and to help strengthen the piezoelectric coefficient. However, stretching may also introduce non-uniform strain into the material, which makes extrinsic factors such as electrostatic interactions more prominent.[25,165]

In contrast to piezoelectricity, electrostatic induction or electromagnetics are known alternatives to piezoelectricity.[198] Unfortunately, these methods have a disadvantage of requiring an external input. This limits the architectural boundaries of future devices. Real competition comes from triboelectric devices that also can be combined into a hybrid piezo-triboelectric device.[199,200] In triboelectric a static electrical charge is generated due to friction of two materials. Certain piezo- and triboelectric devices share similar advantages such as flexibility, stretch-ability, relatively simple design and a general high energy output.[3,81,96,201] Despite piezoelectric limitations, the potency of piezoelectric materials reaches great heights. It will not only be more profoundly available in our daily applications but also for monitoring health.

Author contributions

All authors listed have made substantial, direct and intellectual contributions to the work, and approved it for publication.

Conflicts of interest

There are no conflicts to declare.

References

1 S. Ould Amrouche, D. Rekioua, T. Rekioua and S. Bacha, *Int. J. Hydrogen Energy*, 2016, **41**, 20914–20927.
2 G. Mao, N. Huang, L. Chen and H. Wang, *Sci. Total Environ.*, 2018, **635**, 1081–1090.
3 S. A. Kale, *Renewable energy systems*, 2016.
4 B. Guo, D. Wang, J. Zhou, W. Shi and X. Zhou, *Ocean Eng.*, 2020, **195**, 106791.
5 Y. Ma, Q. Zheng, Y. Liu, B. Shi, X. Xue, W. Ji, Z. Liu, Y. Jin, Y. Zou, Z. An, W. Zhang, X. Wang, W. Jiang, Z. Xu, Z. L. Wang, Z. Li and H. Zhang, *Nano Lett.*, 2016, **16**, 6042–6051.
6 Z. Liu, Y. Ma, H. Ouyang, B. Shi, N. Li, D. Jiang, F. Xie, D. Qu, Y. Zou, Y. Huang, H. Li, C. Zhao, P. Tan, M. Yu, Y. Fan, H. Zhang, Z. L. Wang and Z. Li, *Adv. Funct. Mater.*, 2019, **29**(3), 1807560.
7 T. W. Emans, B. J. Janssen, M. I. Pinkham, C. P. C. Ow, R. G. Evans, J. A. Joles, S. C. Malpas, C. T. P. Krediet and M. P. Koeners, *J. Physiol.*, 2016, **54**, 6287–6300.
8 Z. Li, G. Zhu, R. Yang, A. C. Wang and Z. L. Wang, *Adv. Mater.*, 2010, **22**(23), 2534–2537.
9 C. Dagdeviren, B. D. Yang, Y. Su, P. L. Tran, P. Joe, E. Anderson, J. Xia, V. Doraiswamy, B. Dehdashti, X. Feng, B. Lu, R. Poston, Z. Khalpey, R. Ghaffari, Y. Huang, M. J. Slepian and J. A. Rogers, *Proc. Natl. Acad. Sci. U. S. A.*, 2014, **111**(5), 1927–1932.
10 Z. L. Wang and J. Song, *Science*, 2006, **312**, 242–246.
11 Y. Qi and M. C. McAlpine, *Energy Environ. Sci.*, 2010, **3**, 1275–1285.
12 S. K. Ghosh and D. Mandal, *Appl. Phys. Lett.*, 2016, **109**, 103701.
13 J. Briscoe and S. Dunn, *Nano Energy*, 2015, **14**, 15–29.
14 S. Maiti, S. Kumar Karan, J. Lee, A. Kumar Mishra, B. Bhusan Khatua and J. Kon Kim, *Nano Energy*, 2017, **42**, 282–293.
15 Z. Zhao, T. Wang, J. Shi, B. Zhang, R. Zhang, M. Li and Y. Wen, *Energy Sci. Eng.*, 2019, **7**(6), 2741–2755.
16 X. Li, C. Xu, C. Wang, J. Shao, X. Chen, C. Wang, H. Tian, Y. Wang, Q. Yang, L. Wang and B. Lu, *Nano Energy*, 2017, **40**, 646–654.
17 F. Gao, G. Liu, B. L. H. Chung, H. H. T. Chan and W. H. Liao, *Appl. Phys. Lett.*, 2019, **115**, 033901.
18 D. Berlincourt and H. Jaffe, *Phys. Rev.*, 1958, **111**, 143–148.
19 B. Jaffe, R. S. Roth and S. Marzullo, *J. Appl. Phys.*, 1954, **25**, 809–810.
20 S. Huang, W. A. Yee, W. C. Tjiu, Y. Liu, M. Kotaki, Y. C. F. Boey, J. Ma, T. Liu and X. Lu, *Langmuir*, 2008, **24**(23), 13621–13626.
21 D. Kim, S. A. Han, J. H. Kim, J. H. Lee, S. W. Kim and S. W. Lee, *Adv. Mater.*, 2020, **32**, 1906989.
22 J. Al-Nabulsi, S. El-Sharo, N. Salawy and H. Al-Doori, *J. Med. Eng. Technol.*, 2019, **43**, 255–272.
23 D. M. Shin, S. W. Hong and Y. H. Hwang, *Nanomaterials*, 2020, **10**, 123.
24 F. Ali, W. Raza, X. Li, H. Gul and K. H. Kim, *Nano Energy*, 2019, **57**, 879–902.
25 I. Chae, C. K. Jeong, Z. Ounaies and S. H. Kim, *ACS Appl. Bio Mater.*, 2018, **1**, 936–953.
26 Q. Xu, X. Gao, S. Zhao, Y. N. Liu, D. Zhang, K. Zhou, H. Khanbareh, W. Chen, Y. Zhang and C. Bowen, *Adv. Mater.*, 2021, **33**(27), 2008452.
27 N. Sezer and M. Koç, *Nano Energy*, 2021, **80**, 105567.
28 S. Guerin, S. A. M. Tofail and D. Thompson, *NPG Asia Mater.*, 2019, **11**, 1–5.
29 S. Banerjee, S. Bairagi and S. Wazed Ali, *Ceram. Int.*, 2021, **47**, 16402–16421.
30 P. Muralt, *Encyclopedia of Materials: Science and Technology*, 2001, DOI: 10.1016/b0-08-043152-6/01600-4, pp. 8894–8897.
31 R. Wojnar, in *Piezoelectric Nanomaterials for Biomedical Applications*, ed. G. Ciofani and A. Menciassi, Springer Berlin Heidelberg, Berlin, Heidelberg, 2012, pp. 173–185, DOI: 10.1007/978-3-642-28044-3_6.
32 J. F. Ihlefeld, in *Ferroelectricity in Doped Hafnium Oxide: Materials, Properties and Devices*, 2019, pp. 1–24, DOI: 10.1016/B978-0-08-102430-0.00001-2.
33 T. S. Narasimhamurty, in *Photoelastic and Electro-Optic Properties of Crystals*, ed. T. S. Narasimhamurty, Springer US, Boston, MA, 1981, pp. 333–344, DOI: 10.1007/978-1-4757-0025-1_7.
34 T. Stevenson, D. G. Martin, P. I. Cowin, A. Blumfield, A. J. Bell, T. P. Comyn and P. M. Weaver, *J. Mater. Sci.: Mater. Electron.*, 2015, **26**, 9256–9267.
35 J. Curie and P. Curie, *Bulletin de la Société minéralogique de France*, 1880, DOI: 10.3406/bulmi.1880.1564.
36 J. Valasek, *Phys. Rev.*, 1922, **20**, 639–664.
37 W. P. Mason, *Phys. Rev.*, 1946, **69**, 173–194.
38 M. Ahart, M. Somayazulu, R. E. Cohen, P. Ganesh, P. Dera, H. K. Mao, R. J. Hemley, Y. Ren, P. Liermann and Z. Wu, *Nature*, 2008, **451**, 545–548.
39 A. Muliana, *Int. J. Solids Struct.*, 2011, **48**, 2718–2731.
40 H. Jaffe and D. A. Berlincourt, *Proc. IEEE*, 1965, **53**, 1372–1386.
41 A. R. Hutson, *Phys. Rev. Lett.*, 1960, **4**, 505–507.
42 S. Goel and B. Kumar, *J. Alloys Compd.*, 2020, **816**, 152491.
43 H. A. Wahab, A. A. Salama, A. A. El-Saeid, O. Nur, M. Willander and I. K. Battisha, *Results Phys.*, 2013, **3**, 46–51.
44 S. Jain, N. Karmakar, A. Shah and N. G. Shimpi, *Mater. Sci. Eng. B Solid State Mater. Adv. Technol.*, 2019, **247**, 114381.
45 T. Rueckes, K. Kim, E. Joselevich, G. Y. Tseng, C. L. Cheung and C. M. Lieber, *Science*, 2000, **289**, 94–97.
46 K. Batra, N. Sinha, S. Goel, H. Yadav, A. J. Joseph and B. Kumar, *J. Alloys Compd.*, 2018, **767**, 1003–1011.
47 L. Egerton and S. E. Koonce, *J. Am. Ceram. Soc.*, 1955, **38**, 412–418.
48 J. P. Praveen, T. Karthik, A. R. James, E. Chandrakala, S. Asthana and D. Das, *J. Eur. Ceram. Soc.*, 2015, **35**, 1785–1798.

49 M. Acosta, N. Novak, V. Rojas, S. Patel, R. Vaish, J. Koruza, G. A. Rossetti and J. Rödel, *Appl. Phys. Rev.*, 2017, **4**, 041305.
50 Y. Wang, H. Cheng, J. Yan, N. Chen, P. Yan, F. Yang and J. Ouyang, *Materialia*, 2019, **5**, 100228.
51 Y. Qi and M. C. McAlpine, *Energy Environ. Sci.*, 2010, **3**, 1275–1285.
52 I. Kanno, H. Kotera and K. Wasa, *Sens. Actuators, A*, 2003, **107**, 68–74.
53 C. Zhao, H. Wu, F. Li, Y. Cai, Y. Zhang, D. Song, J. Wu, X. Lyu, J. Yin, D. Xiao, J. Zhu and S. J. Pennycook, *J. Am. Chem. Soc.*, 2018, **140**, 15252–15260.
54 Y. Saito, H. Takao, T. Tani, T. Nonoyama, K. Takatori, T. Homma, T. Nagaya and M. Nakamura, *Nature*, 2004, **432**, 84–87.
55 X. Lv, J. Wu, J. Zhu, D. Xiao and X. Zhangb, *J. Eur. Ceram. Soc.*, 2018, **38**, 85–94.
56 P. Li, J. Zhai, B. Shen, S. Zhang, X. Li, F. Zhu and X. Zhang, *Adv. Mater.*, 2018, **30**, 1705171.
57 B. Gamboa, A. Bhalla and R. Guo, *Ferroelectrics*, 2020, **555**, 118–123.
58 M. Algueró, B. L. Cheng, F. Guiu, M. J. Reece, M. Poole and N. Alford, *J. Eur. Ceram. Soc.*, 2001, **21**, 1437–1440.
59 T. Starner, *IBM Syst. J.*, 1996, **35**, 618–629.
60 A. G. Tobin and E. Pak, *Proc. SPIE*, 1993, **1916**, 78–86.
61 Y. Qi, J. Kim, T. D. Nguyen, B. Lisko, P. K. Purohit and M. C. McAlpine, *Nano Lett.*, 2011, **11**(3), 1331–1336.
62 S. I. Park, J. H. Ahn, X. Feng, S. Wang, Y. Huang and J. A. Rogers, *Adv. Funct. Mater.*, 2008, **18**, 2673–2684.
63 H. Jaffe, *J. Am. Ceram. Soc.*, 1958, **41**, 494–498.
64 G. H. Haertling, *J. Am. Ceram. Soc.*, 1999, **82**, 797–818.
65 W. Liu and X. Ren, *Phys. Rev. Lett.*, 2009, **103**, 257602.
66 I. Bhaumik, G. Singh, S. Ganesamoorthy, R. Bhatt, A. K. Karnal, V. S. Tiwari and P. K. Gupta, *J. Cryst. Growth*, 2013, **375**, 20–25.
67 P. Wang, Y. Li and Y. Lu, *J. Eur. Ceram. Soc.*, 2011, **31**, 2005–2012.
68 Y. Tan, J. Zhang, Y. Wu, C. Wang, V. Koval, B. Shi, H. Ye, R. McKinnon, G. Viola and H. Yan, *Sci. Rep.*, 2015, **5**, 9953.
69 L. Zhao, B. P. Zhang, P. F. Zhou, L. F. Zhu and J. F. Li, *J. Eur. Ceram. Soc.*, 2015, **35**, 533–540.
70 S. A. Khan, F. Akram, J. Bae, T. Ahmed, T. K. Song, Y. S. Sung, M. H. Kim and S. Lee, *Solid State Sci.*, 2019, **98**, 106040.
71 J. Wu, H. Tao, Y. Yuan, X. Lv, X. Wang and X. Lou, *RSC Adv.*, 2015, **5**, 14575–14583.
72 F. Rubio-Marcos, R. López-Juárez, R. E. Rojas-Hernandez, A. Del Campo, N. Razo-Pérez and J. F. Fernandez, *ACS Appl. Mater. Interfaces*, 2015, **7**, 23080–23088.
73 Y. Huan, X. Wang, Z. Shen, J. Kim, H. Zhou and L. Li, *J. Am. Ceram. Soc.*, 2014, **97**, 700–703.
74 Y. A. Genenko, J. Glaum, M. J. Hoffmann and K. Albe, *Mater. Sci. Eng. B Solid State Mater. Adv. Technol.*, 2015, **192**, 52–82.
75 C. Zhou, H. Lin, Q. He, L. Xu, M. Worku, M. Chaaban, S. Lee, X. Shi, M. H. Du and B. Ma, *Mater. Sci. Eng., R*, 2019, **137**, 38–65.
76 D. Wang, M. Wright, N. K. Elumalai and A. Uddin, *Sol. Energy Mater. Sol. Cells*, 2016, **147**, 255–275.
77 Y. M. You, W. Q. Liao, D. Zhao, H. Y. Ye, Y. Zhang, Q. Zhou, X. Niu, J. Wang, P. F. Li, D. W. Fu, Z. Wang, S. Gao, K. Yang, J. M. Liu, J. Li, Y. Yan and R. G. Xiong, *Science*, 2017, **357**, 306–309.
78 W. Q. Liao, D. Zhao, Y. Y. Tang, Y. Zhang, P. F. Li, P. P. Shi, X. G. Chen, Y. M. You and R. G. Xiong, *Science*, 2019, **363**, 1206–1210.
79 M. Coll, A. Gomez, E. Mas-Marza, O. Almora, G. Garcia-Belmonte, M. Campoy-Quiles and J. Bisquert, *J. Phys. Chem. Lett.*, 2015, **6**, 1408–1413.
80 X. Wu, H. Yu, N. Li, F. Wang, H. Xu and N. Zhao, *J. Phys. Chem. C*, 2015, **119**, 1253–1259.
81 L. Yang, S. Chi, S. Dong, F. Yuan, Z. Wang, J. Lei, L. Bao, J. Xiang and J. Wang, *Nano Energy*, 2020, **67**, 104220.
82 J. Gomes, J. S. Nunes, V. Sencadas and S. Lanceros-Mendez, *Smart Mater. Struct.*, 2010, **19**, 065010.
83 M. Poulsen and S. Ducharme, *IEEE Trans. Dielectr. Electr. Insul.*, 2010, **17**, 1028–1035.
84 C. A. Sperati and H. W. Starkweather Jr, *Fortschr. Hochpolym.-Forsch.*, 1961, **2**, 465–495.
85 M. Kutz, *Applied Plastics Engineering Handbook: Processing, Materials, and Applications: Second Edition*, 2016.
86 C. Chen, Z. Bai, Y. Cao, M. Dong, K. Jiang, Y. Zhou, Y. Tao, S. Gu, J. Xu, X. Yin and W. Xu, *Compos. Sci. Technol.*, 2020, **192**, 108100.
87 S. S. Won, M. Sheldon, N. Mostovych, J. Kwak, B. S. Chang, C. W. Ahn, A. I. Kingon, I. W. Kim and S. H. Kim, *Appl. Phys. Lett.*, 2015, **107**, 202901.
88 R. A. Surmenev, T. Orlova, R. V. Chernozem, A. A. Ivanova, A. Bartasyte, S. Mathur and M. A. Surmeneva, *Nano Energy*, 2019, **62**, 475–506.
89 A. Talbourdet, F. Rault, G. Lemort, C. Cochrane, E. Devaux and C. Campagne, *Smart Mater. Struct.*, 2018, **27**, 075010.
90 S. S. Chauhan, U. M. Bhatt, P. Gautam, S. Thote, M. M. Joglekar and S. K. Manhas, *Sens. Actuators, A*, 2020, **304**, 111879.
91 S. Park, Y. Kim, H. Jung, J. Y. Park, N. Lee and Y. Seo, *Sci. Rep.*, 2017, **7**, 17290.
92 F. J. Baltá Calleja, A. González Arche, T. A. Ezquerra, C. Santa Cruz, F. Batallán, B. Frick and E. López Cabarcos, *Journal*, 1993, **108**, X-48.
93 T. Wang, Z. Feng, Y. Song and X. Chen, *Dent. Mater.*, 2007, **23**, 450–453.
94 L. Persano, C. Dagdeviren, Y. Su, Y. Zhang, S. Girardo, D. Pisignano, Y. Huang and J. A. Rogers, *Nat. Commun.*, 2013, **4**, 1633.
95 Z. H. Liu, C. T. Pan, L. W. Lin, J. C. Huang and Z. Y. Ou, *Smart Mater. Struct.*, 2014, **23**, 025003.
96 X. Wang, B. Yang, J. Liu, Y. Zhu, C. Yang and Q. He, *Sci. Rep.*, 2016, **6**, 36409.
97 W. H. Liew, M. S. Mirshekarloo, S. Chen, K. Yao and F. E. H. Tay, *Sci. Rep.*, 2015, **5**, 09790.
98 T. Sharma, S. S. Je, B. Gill and J. X. J. Zhang, *Sens. Actuators, A*, 2012, **177**, 87–92.
99 Y. A. Yildirim, A. Toprak and O. Tigli, *J. Microelectromech. Syst.*, 2018, **27**, 86–94.

100 Z. Ounaies, J. A. Young and J. S. Harrison, *Journal*, 1999, **726**, 88–103.
101 S. Miyata, M. Yoshikawa, S. Tasaka and M. Ko, *Polym. J.*, 1980, **12**, 857–860.
102 D. Singh, A. Choudhary and A. Garg, *ACS Appl. Mater. Interfaces*, 2018, **10**, 2793–2800.
103 J. Li, C. Zhao, K. Xia, X. Liu, D. Li and J. Han, *Appl. Surf. Sci.*, 2019, **463**, 626–634.
104 N. A. Hoque, P. Thakur, S. Roy, A. Kool, B. Bagchi, P. Biswas, M. M. Saikh, F. Khatun, S. Das and P. P. Ray, *ACS Appl. Mater. Interfaces*, 2017, **9**, 23048–23059.
105 S. Garain, T. Kumar Sinha, P. Adhikary, K. Henkel, S. Sen, S. Ram, C. Sinha, D. Schmeißer and D. Mandal, *ACS Appl. Mater. Interfaces*, 2015, **7**, 1298–1307.
106 C. Mota, M. Labardi, L. Trombi, L. Astolfi, M. D'Acunto, D. Puppi, G. Gallone, F. Chiellini, S. Berrettini, L. Bruschini and S. Danti, *Mater. Des.*, 2017, **122**, 206–219.
107 C. K. Jeong, C. Baek, A. I. Kingon, K. I. Park and S. H. Kim, *Small*, 2018, **14**, 1704022.
108 S. Bairagi and S. W. Ali, *Energy*, 2020, **198**, 117385.
109 S. Guerin, T. A. M. Syed and D. Thompson, *Nanoscale*, 2018, **10**, 9653–9663.
110 A. Gruverman, B. J. Rodriguez and S. V. Kalinin, *Scanning Probe Microsc.*, 2007, **2**, 615–633.
111 A. Šutka, P. C. Sherrell, N. A. Shepelin, L. Lapčinskis, K. Mālnieks and A. V. Ellis, *Adv. Mater.*, 2020, **32**, 2002979.
112 P. Jiang, F. Yan, E. Nasr Esfahani, S. Xie, D. Zou, X. Liu, H. Zheng and J. Li, *ACS Biomater. Sci. Eng.*, 2017, **3**, 1827–1835.
113 H. Y. Jiang, F. Yen, C. W. Huang, R. B. Mei and L. Chen, *AIP Adv.*, 2017, **7**, 045215.
114 H. Ueda and E. Fakada, *Jpn. J. Appl. Phys., Part 1*, 1971, **10**, 1650–1651.
115 A. Stapleton, M. R. Noor, J. Sweeney, V. Casey, A. L. Kholkin, C. Silien, A. A. Gandhi, T. Soulimane and S. A. M. Tofail, *Appl. Phys. Lett.*, 2017, **111**, 142902.
116 A. Stapleton, M. S. Ivanov, M. R. Noor, C. Silien, A. A. Gandhi, T. Soulimane, A. L. Kholkin and S. A. M. Tofail, *Ferroelectrics*, 2018, **525**, 135–145.
117 Y. Liu, Y. Wang, M. J. Chow, N. Q. Chen, F. Ma, Y. Zhang and J. Li, *Phys. Rev. Lett.*, 2013, **110**, 1–5.
118 Y. Liu, H. L. Cai, M. Zelisko, Y. Wang, J. Sun, F. Yan, F. Ma, P. Wang, Q. N. Chen, H. Zheng, X. Meng, P. Sharma, Y. Zhang and J. Li, *Proc. Natl. Acad. Sci. U. S. A.*, 2014, **111**, E2780–E2786.
119 E. Fukada and I. Yasuda, *Jpn. J. Appl. Phys., Part 1*, 1964, **3**, 502B.
120 E. Fukada and H. Ueda, *Jpn. J. Appl. Phys., Part 1*, 1970, **9**, 844–845.
121 S. Guerin, A. Stapleton, D. Chovan, R. Mouras, M. Gleeson, C. McKeown, M. R. Noor, C. Silien, F. M. F. Rhen, A. L. Kholkin, N. Liu, T. Soulimane, S. A. M. Tofail and D. Thompson, *Nat. Mater.*, 2018, **17**, 180–186.
122 E. Fukada, *Wood Sci. Technol.*, 1968, **2**, 299–307.
123 E. Fukada, *J. Phys. Soc. Jpn.*, 1955, **10**, 149–154.
124 C. M. Lee, K. Kafle, D. W. Belias, Y. B. Park, R. E. Glick, C. H. Haigler and S. H. Kim, *Cellulose*, 2015, **22**, 971–989.
125 K. Kafle, R. Shi, C. M. Lee, A. Mittal, Y. B. Park, Y. H. Sun, S. Park, V. Chiang and S. H. Kim, *Cellulose*, 2014, **21**, 2219–2231.
126 B. Frka-Petesic, B. Jean and L. Heux, *Europhys. Lett.*, 2014, **107**, 28006.
127 S. Rajala, T. Siponkoski, E. Sarlin, M. Mettänen, M. Vuoriluoto, A. Pammo, J. Juuti, O. J. Rojas, S. Franssila and S. Tuukkanen, *ACS Appl. Mater. Interfaces*, 2016, **8**, 15607–15614.
128 S. Yun, J. H. Kim, Y. Li and J. Kim, *J. Appl. Phys.*, 2008, **103**, 083301.
129 J. Wang, J. Wang, C. Carlos, Z. Zhang, J. Li, Y. Long, F. Yang, Y. Dong, X. Qiu, Y. Qian and X. Wang, *ACS Appl. Mater. Interfaces*, 2020, **12**, 26399–26404.
130 I. Chae, S. M. Q. Bokhari, X. Chen, R. Zu, K. Liu, A. Borhan, V. Gopalan, J. M. Catchmark and S. H. Kim, *Carbohydr. Polym.*, 2021, **255**, 117328.
131 G. Y. Yun, H. S. Kim, J. Kim, K. Kim and C. Yang, *Sens. Actuators, A*, 2008, **141**, 530–535.
132 J. Leppiniemi, P. Lahtinen, A. Paajanen, R. Mahlberg, S. Metsä-Kortelainen, T. Pinomaa, H. Pajari, I. Vikholm-Lundin, P. Pursula and V. P. Hytönen, *ACS Appl. Mater. Interfaces*, 2017, **9**, 21959–21970.
133 A. Hänninen, E. Sarlin, I. Lyyra, T. Salpavaara, M. Kellomäki and S. Tuukkanen, *Carbohydr. Polym.*, 2018, **202**, 418–424.
134 E. S. Choi, H. C. Kim, R. M. Muthoka, P. S. Panicker, D. O. Agumba and J. Kim, *Compos. Sci. Technol.*, 2021, **209**, 108795.
135 O. M. Vanderfleet and E. D. Cranston, *Nat. Rev. Mater.*, 2021, **6**, 124–144.
136 D. Lasrado, S. Ahankari and K. Kar, *J. Appl. Polym. Sci.*, 2020, **137**, 48959.
137 P. K. Annamalai, A. K. Nanjundan, D. P. Dubal and J. B. Baek, *Adv. Mater. Technol.*, 2021, **6**(2021), 2001164.
138 D. Vasilescu, R. Cornillon and G. Mallet, *Nature*, 1970, **225**, 635.
139 V. V. Lemanov, S. N. Popov and G. A. Pankova, *Phys. Solid State*, 2011, **53**, 1191–1193.
140 D. Denning, J. I. Kilpatrick, E. Fukada, N. Zhang, S. Habelitz, A. Fertala, M. D. Gilchrist, Y. Zhang, S. A. M. Tofail and B. J. Rodriguez, *ACS Biomater. Sci. Eng.*, 2017, **3**, 929–935.
141 M. Minary-Jolandan and M. F. Yu, *Appl. Phys. Lett.*, 2010, **97**, 153127.
142 J. Reyes-Gasga, M. Galindo-Mentle, E. Brès, N. Vargas-Becerril, E. Orozco, A. Rodríguez-Gómez and R. García-García, *J. Phys. Chem. Solids*, 2020, **136**, 109140.
143 S. Ghosh, B. Z. Mei, V. Lubkin, J. I. Scheinbeim, B. A. Newman, P. Kramer, G. Bennett and N. Feit, *J. Biomed. Mater. Res.*, 1998, **39**, 453–457.
144 B. Y. Lee, J. Zhang, C. Zueger, W. J. Chung, S. Y. Yoo, E. Wang, J. Meyer, R. Ramesh and S. W. Lee, *Nat. Nanotechnol.*, 2012, **7**, 351–356.
145 D. M. Shin, H. J. Han, W. G. Kim, E. Kim, C. Kim, S. W. Hong, H. K. Kim, J. W. Oh and Y. H. Hwang, *Energy Environ. Sci.*, 2015, **8**, 3198–3203.

146 J. H. Lee, J. H. Lee, J. Xiao, M. S. Desai, X. Zhang and S. W. Lee, *Nano Lett.*, 2019, **19**, 2661–2667.
147 P. Hu, S. Hu, Y. Huang, J. R. Reimers, A. M. Rappe, Y. Li, A. Stroppa and W. Ren, *J. Phys. Chem. Lett.*, 2019, **10**, 1319–1324.
148 A. Heredia, V. Meunier, I. K. Bdikin, J. Gracio, N. Balke, S. Jesse, A. Tselev, P. K. Agarwal, B. G. Sumpter, S. V. Kalinin and A. L. Kholkin, *Adv. Funct. Mater.*, 2012, **22**, 2996–3003.
149 S. Guerin, S. A. M. Tofail and D. Thompson, *Cryst. Growth Des.*, 2018, **18**, 4844–4848.
150 Y. Sun, K. Y. Zeng and T. Li, *Sci. China: Phys., Mech. Astron.*, 2020, **63**, 278701.
151 M. Nair, Y. Calahorra, S. Kar-Narayan, S. M. Best and R. E. Cameron, *Nanoscale*, 2019, **11**, 15120–15130.
152 A. A. Marino and B. D. Gross, *Arch. Oral Biol.*, 1989, **34**, 507–509.
153 M. Minary-Jolandan and M. F. Yu, *ACS Nano*, 2009, **3**, 1859–1863.
154 Z. Tylczyski, A. Sterczyska and M. Wiesner, *J. Phys.: Condens. Matter*, 2011, **23**, 355901.
155 Y. Zhang, A. A. Gandhi, J. Zeglinski, M. Gregor and S. A. M. Tofail, *IEEE Trans. Dielectr. Electr. Insul.*, 2012, **19**, 1151–1157.
156 E. Fukada and I. Yasuda, *J. Phys. Soc. Jpn.*, 1957, **12**, 1158–1162.
157 A. H. Rajabi, M. Jaffe and T. L. Arinzeh, *Acta Biomater.*, 2015, **24**, 12–23.
158 M. Minary-Jolandan and M. F. Yu, *Nanotechnology*, 2009, **20**, 085706.
159 A. C. Jayasuriya, J. I. Scheinbeim, V. Lubkin, G. Bennett and P. Kramer, *J. Biomed. Mater. Res.*, 2003, **66**, 260–265.
160 A. C. Jayasuriya, S. Ghosh, J. I. Scheinbeim, V. Lubkin, G. Bennett and P. Kramer, *Biosens. Bioelectron.: X*, 2003, **18**, 381–387.
161 S. K. Ghosh and D. Mandal, *Nano Energy*, 2016, **28**, 356–365.
162 N. R. Alluri, N. Prashanth, M. Joseph, G. Khandelwal, V. Vivekananthan and S.-j. Kim, *Nano Energy*, 2020, **73**, 104767.
163 A. Gaur, S. Tiwari, C. Kumar and P. Maiti, *Energy Rep.*, 2020, **6**, 490–496.
164 D. Jiang, B. Shi, H. Ouyang, Y. Fan, Z. L. Wang, Z. M. Chen and Z. Li, *Mater. Today Energy*, 2020, **16**, 100386.
165 J. Li, Y. Long, F. Yang and X. Wang, *Curr. Opin. Solid State Mater. Sci.*, 2020, **24**, 100806.
166 X. Cheng, X. Xue, Y. Ma, M. Han, W. Zhang, Z. Xu, H. Zhang and H. Zhang, *Nano Energy*, 2016, **22**, 453–460.
167 C. Wang, S. Wang, Z. Gao and X. Wang, *Appl. Energy*, 2019, **251**, 113383.
168 L. Guo and Q. Lu, *Renew. Sustain. Energy Rev.*, 2017, **72**, 761–773.
169 Y. Tianchen, Y. Jian, S. Ruigang and L. Xiaowei, *Smart Mater. Struct.*, 2014, **23**, 125046.
170 F. Faisal, N. Wu and K. Kapoor, *Proc. SPIE*, 2016, **9799**, 97992Q.
171 P. Liu, Y. Hu, B. Geng and D. Xu, *J. Mater. Res. Technol.*, 2020, **9**, 3511–3519.
172 P. Liu, Y. Hu, Y. Chen, B. Geng and D. Xu, *Constr. Build. Mater.*, 2020, **235**, 117495.
173 J. S. Lee, K. Y. Shin, O. J. Cheong, J. H. Kim and J. Jang, *Sci. Rep.*, 2015, **5**, 7887.
174 M. Zhu, M. Lou, I. Abdalla, J. Yu, Z. Li and B. Ding, *Nano Energy*, 2020, **69**, 104429.
175 H. Yuan, T. Lei, Y. Qin, J. H. He and R. Yang, *J. Phys. D: Appl. Phys.*, 2019, **51**, 194002.
176 V. Nguyen, S. Kelly and R. Yang, *APL Mater.*, 2017, **5**, 074108.
177 W. A. Yee, M. Kotaki, Y. Liu and X. Lu, *Polymer*, 2007, **48**, 512–521.
178 S. K. Karan, S. Maiti, S. Paria, A. Maitra, S. K. Si, J. K. Kim and B. B. Khatua, *Mater. Today Energy*, 2018, **9**, 114–125.
179 A. Maitra, S. K. Karan, S. Paria, A. K. Das, R. Bera, L. Halder, S. K. Si, A. Bera and B. B. Khatua, *Nano Energy*, 2017, **40**, 633–645.
180 S. K. Ghosh and D. Mandal, *ACS Sustainable Chem. Eng.*, 2017, **5**, 8836–8843.
181 S. K. Ghosh, P. Adhikary, S. Jana, A. Biswas, V. Sencadas, S. D. Gupta, B. Tudu and D. Mandal, *Nano Energy*, 2017, **36**, 166–175.
182 V. Vivekananthan, N. R. Alluri, Y. Purusothaman, A. Chandrasekhar, S. Selvarajan and S. J. Kim, *ACS Appl. Mater. Interfaces*, 2018, **10**, 18650–18656.
183 D. I. Zeugolis, G. R. Paul and G. Attenburrow, *J. Biomed. Mater. Res.*, 2009, **89**, 895–908.
184 C. R. West and A. E. Bowden, *Ann. Biomed. Eng.*, 2012, **40**, 1568–1574.
185 J. S. Moon, Y. Lee, D. M. Shin, C. Kim, W. G. Kim, M. Park, J. Han, H. Song, K. Kim and J. W. Oh, *Chem. Asian J.*, 2016, **11**, 3097–3101.
186 Y. C. Shin, C. Kim, S. J. Song, S. Jun, C. S. Kim, S. W. Hong, S. H. Hyon, D. W. Han and J. W. Oh, *Nanotheranostics*, 2018, **2**, 144–156.
187 I. S. Raja, C. Kim, S. J. Song, Y. C. Shin, M. S. Kang, S. H. Hyon, J. W. Oh and D. W. Han, *Nanomaterials*, 2019, **9**, 1014.
188 R. M. Street, T. Huseynova, X. Xu, P. Chandrasekaran, L. Han, W. Y. Shih, W. H. Shih and C. L. Schauer, *Carbohydr. Polym.*, 2018, **195**, 218–224.
189 T. Ibn-Mohammed, I. M. Reaney, S. C. L. Koh, A. Acquaye, D. C. Sinclair, C. A. Randall, F. H. Abubakar, L. Smith, G. Schileo and L. Ozawa-Meida, *J. Eur. Ceram. Soc.*, 2018, **38**, 4922–4938.
190 J. Koruza, A. J. Bell, T. Frömling, K. G. Webber, K. Wang and J. Rödel, *J. Materiomics*, 2018, **4**, 13–26.
191 M. H. Chung, S. Yoo, H. J. Kim, J. Yoo, S. Y. Han, K. H. Yoo and H. Jeong, *Sci. Rep.*, 2019, **9**, 6581.
192 L. Zhang, S. R. Oh, T. C. Wong, C. Y. Tan and K. Yao, *IEEE Trans. Ultrason. Ferroelectrics Freq. Contr.*, 2013, **60**, 2013–2020.
193 V. T. Rathod, *Electronics*, 2019, **8**, 169.
194 A. Mohebbi, F. Mighri, A. Ajji and D. Rodrigue, *Polym. Adv. Technol.*, 2017, **28**, 476–483.
195 N. Soin, T. H. Shah, S. C. Anand, J. Geng, W. Pornwannachai, P. Mandal, D. Reid, S. Sharma,

R. L. Hadimani, D. V. Bayramol and E. Siores, *Energy Environ. Sci.*, 2014, **7**, 1670–1679.

196 J. Kim, S. Yun, S. K. Mahadeva, K. Yun, S. Y. Yang and M. Maniruzzaman, *Sensors*, 2010, **10**, 1473–1485.

197 A. Rosengren, L. Faxius, N. Tanaka, M. Watanabe and L. M. Bjursten, *J. Biomed. Mater. Res.*, 2005, **75**, 115–122.

198 D. A. Wang and K. H. Chang, *Microelectron. J.*, 2010, **41**, 356–364.

199 S. Cherumannil Karumuthil, S. P. Rajeev and S. Varghese, *Nano Energy*, 2017, **40**, 487–494.

200 Z. Li, Z. Saadatnia, Z. Yang and H. Naguib, *Energy Convers. Manage.*, 2018, **174**, 188–197.

201 Q. Zheng, B. Shi, Z. Li and Z. L. Wang, *Adv. Sci.*, 2017, **4**, 1700029.